Journal of Biochemical and Molecular Toxicology

WILEY

RESEARCH ARTICLE OPEN ACCESS

L-Securinine Induces ROS-Dependent Apoptosis on Pancreatic Cancer Cells via the PI3K/AKT/mTOR Signaling Pathway

Ioanna A. Anastasiou[1,2] | Panagiotis Sarantis[3] | Eleni Rebelos[1,4] | Ioanna Eleftheriadou[1] | Konstantinos N. Tentolouris[1,2] | Athanasia Katsaouni[2] | Evangelos Koustas[3] | Vasileia Kokala[1] | Michalis V. Karamouzis[3] | Nikolaos Tentolouris[1]

[1]First Department of Propaedeutic Internal Medicine, Diabetes Center, Medical School, National and Kapodistrian University of Athens, Laiko General Hospital, Athens, Greece | [2]Department of Pharmacology, Medical School, National and Kapodistrian University of Athens, Athens, Greece | [3]Molecular Oncology Unit, Department of Biological Chemistry, Medical School, National and Kapodistrian University of Athens, Greece | [4]Turku PET Centre, University of Turku, Turku, Finland

Correspondence: Ioanna A. Anastasiou (anastasiouiwanna@gmail.com)

Received: 30 April 2024 | **Revised:** 3 September 2024 | **Accepted:** 18 October 2024

Funding: This study was supported by National and Kapodistrian University of Athens, Greece's Special Account for Research Grants (SARG) (SARG 70/3/16125).

Keywords: apoptosis | in vitro studies | L-securinine | pancreatic cancer | reactive oxygen species

ABSTRACT

Accumulating evidence has shown that L-securinine can, in certain circumstances, suppress tumor development by elevating reactive oxygen species (ROS) levels. The current work set out to examine L-securinine's apoptotic effects on HuP-T3 cells as well as any potential underlying molecular mechanism(s) that could explain its action as an anticancer agent. In this study, we used 1.2B4 cells as a control human cell line to verify our findings. Hup-T3 and 1.2B4 cells were cultured with a medium containing the following dilutions of L-securinine: 1–10 μM for up to 72 h. We examined the viability and proliferation levels of cells in both cell lines. Then, we measured only 1.2B4 insulin levels and content. We also quantified cell apoptosis, cell cycle levels, and the intracellular reactive oxygen species on HuP-T3 and 1.2B4. Afterwards, we performed a real-time quantitative polymerase chain reaction and western blot analysis. Our results demonstrated that L-securinine inhibited both proliferation and growth of Hup-T3 cells, showing inhibitory and antiproliferative activity in comparison with the control group. In addition, L-securinine had no impact on the proliferation and growth of 1.2B4 cells, nor on their insulin levels and content. By boosting ROS production, and inhibiting the PI3K/AKT/mTOR signaling pathway, L-securinine induced apoptosis on HuP-T3 cells. Pancreatic cancer was successfully inhibited by L-securinine in vitro. L-securinine triggers ROS-dependent apoptosis on pancreatic cancer cells while inhibiting the PI3K/AKT/mTOR signaling pathway. These findings suggest that L-securinine holds promise as a potential lead for future drug development in the fight against pancreatic adenocarcinoma.

1 | Introduction

Pancreatic ductal adenocarcinoma (PDAC) is the third most prevalent cause of cancer-related mortality in the United States [1]. The Surveillance, Epidemiology, and End Result Program (SEER) reports that around 57,600 new cases were identified in 2020, resulting in 47,050 deaths [2]. This disease has an unfavorable prognosis because of its rapid systemic dissemination and rapid local development. Ten to fifteen percent of patients have a local disease, 25%–30%

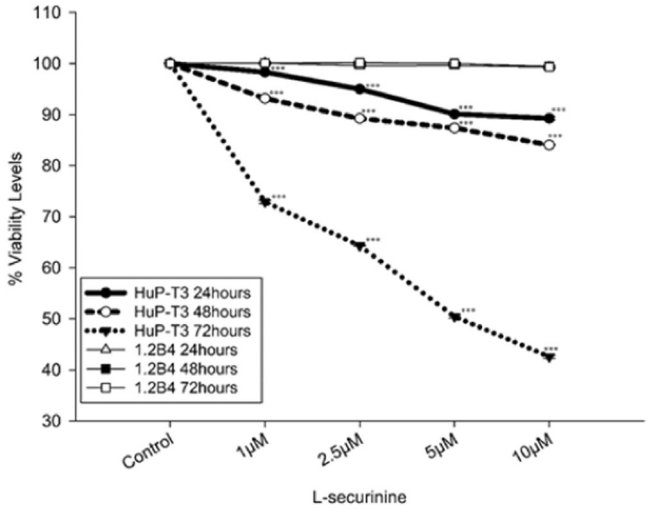

FIGURE 1 | Cell viability levels of HuP-T3 and 1.2B4. L-securinine inhibits the growth of HuP-T3, whereas no change was observed in cell viability levels of 1.2B4. Cell viability was determined by MTT assay. HuP-T3 and 1.2B4 cells were cultured with L-securinine in several concentrations (control = 0.1% v/v vehicle of DMSO, 1, 2.5, 5, and 10 μM) for 24, 48 and 72 h. The data are expressed as mean ± SD of three independent experiments ($N = 3$). Statistical significance was determined by one-way ANOVA followed by the Dunnett's T3 post hoc test; where *p-value < 0.05; **p-value < 0.01; ***p-value < 0.001 in comparison with control group. ANOVA, analysis of variance; DMSO, dimethyl sulfoxide; MTT, 3-(4,5-dimethylthiazol-2-yl)-2,5-diphenyltetrazolium bromide; SD, standard deviation.

have regional disease, and 50%–60% of patients have distant metastatic disease [3]. The tumor's respectability determines the course of treatment and prognosis for individuals with local or regional disease [1].

Natural components play a critical role in modern drug development and represent a source of molecules able to affect cell signal transduction pathways. Plants have been used in the treatment of diseases, and more than 35,000 species have been screened for medicinal properties [4]. Due to their high activity and low cytotoxicity as anticancer medicines, an increasing number of naturally bioactive chemicals discovered in traditional Chinese medicine have drawn significant attention from researchers for use in cancer therapy [4]. One of Securinega suffruticosa's main plant-derived alkaloids, L-securinine, has a variety of biological effects, including antibacterial and antimalarial ones [5]. It has a long history of being used in folk medicine to treat neurological disorders [6]. In general, recent pharmacological research has demonstrated that securinine [7], one of the optical isomers of L-securinine [8], plays a crucial role in antitumor activity in human cancer cell lines, making it a prospective target for the development of future cancer treatments [5].

In one study, researchers examined the anticancer and antimitotic properties of the plant-derived alkaloid L-securinine and how it affects cellular microtubule architecture and binds to isolated goat brain tubulin in vitro [9]. Their results showed that treating L-securinine induced a mitochondrial-dependent reactive oxygen species (ROS) response in HeLa cells, enhancing L-securinine's cytotoxic effect. They also indicated that L-securinine induced apoptosis in MCF-7 cells through the p53-dependent pathway [9]. L-securinine also inhibits the spread of cancer cells and increases autophagy and cell death via regulating the signal pathways of Wnt, phosphatidylinositol-3-kinase/protein kinase B/mammalian target of rapamycin, and Janus kinase—signal transducer and activator of transcription [10]. Thanks to these properties, it has been shown that L-securinine is capable of killing a variety of human cancer cells, such as leukemia, prostate, cervical, breast, lung, and colon cancer cells [10]. There are no in vivo data about anticancer activity of L-securinine on pancreatic adenocarcinoma, but there are in vitro and in vivo data with natural drugs which mediated simultaneous targeting of the PI3K/Akt/mTOR pathway reduced PDAC tumor growth and improved survival in the genetically engineered mouse model (GEMM) of PDAC [11]. In eukaryotic cells, the PI3K/AKT/mTOR signaling pathway is a highly conserved signal transduction network contributing to cell growth, survival, and cycle progression [12].

Although L-securinine has a wide range of pharmacological effects, no data exist on its potential antitumor action on human pancreatic cancer cells, Thus, the goal of the current study is to determine the effect of L-securinine on pancreatic cancer cells and to elucidate the underlying mechanisms of its anticancer action.

2 | Material and Methods

2.1 | Cell Culture

HuP-T3 (RRID:CVCL_1299) is a human pancreatic carcinoma cell line derived from the ascites of pancreatic cancer patients suffering from carcinomatous peritonitis. 1.2B4 (RRID: CVCL_2258) is a human hybrid pancreatic islet cell line that produces pure insulin-secreting cells when stimulated [13]. 1.2B4 produced by electrofusion of HuP-T3 with a primary culture of human pancreatic islets [13]. The HuP-T3 cell line was cultured in Minimum Essential Medium Eagle Alpha Modification (MEM, Sigma-Aldrich Co., St Louis, MO, USA), and the 1.2B4 cell line was cultured in RPMI-1640 Medium containing 2mM L-glutamine (Thermo Fisher Scientific, Waltham, MA, USA). All cell culture media were supplemented with 10% heat-inactivated fetal bovine serum (FBS; Sigma-Aldrich Co., St Louis, MO, USA) and 1% of a mixture of penicillin/streptomycin (1000 U/mL; 10 mg/mL, Thermo Scientific, Fremont, CA, USA). Cells were subcultured once they had reached 70%–80% confluence. Cells were obtained from either the American Type Culture Collection (ATCC) or American Type European Collection of Authenticated Cell Cultures (ECACC). They were all maintained in a humidified atmosphere containing 95% O_2 and 5% CO_2 at 37°C for a maximum of 4–5 weeks.

In summary, L-securinine (1, 2.5, 5, and 10 μg/mL) was added to the HuP-T3 and 1.2B4 and incubated for 24–72 h. For experiments, cells were seeded at the density of 5.0×10^3 cells/well in 96-well plates, 1.5×10^5 cells/well in 24-well plates, and in eight-chamber slides, 1.0×10^6 cells/well in six-well plates. The control was a fresh culture medium with 0.1% v/v vehicle of dimethyl sulfoxide (DMSO). The concentrations of L-securinine were referred to in previous studies [14]. L-securinine from *Hypericum perforatum* (≥ 98% purity, 5610-40-2, Sigma Aldrich, United States) was dissolved in

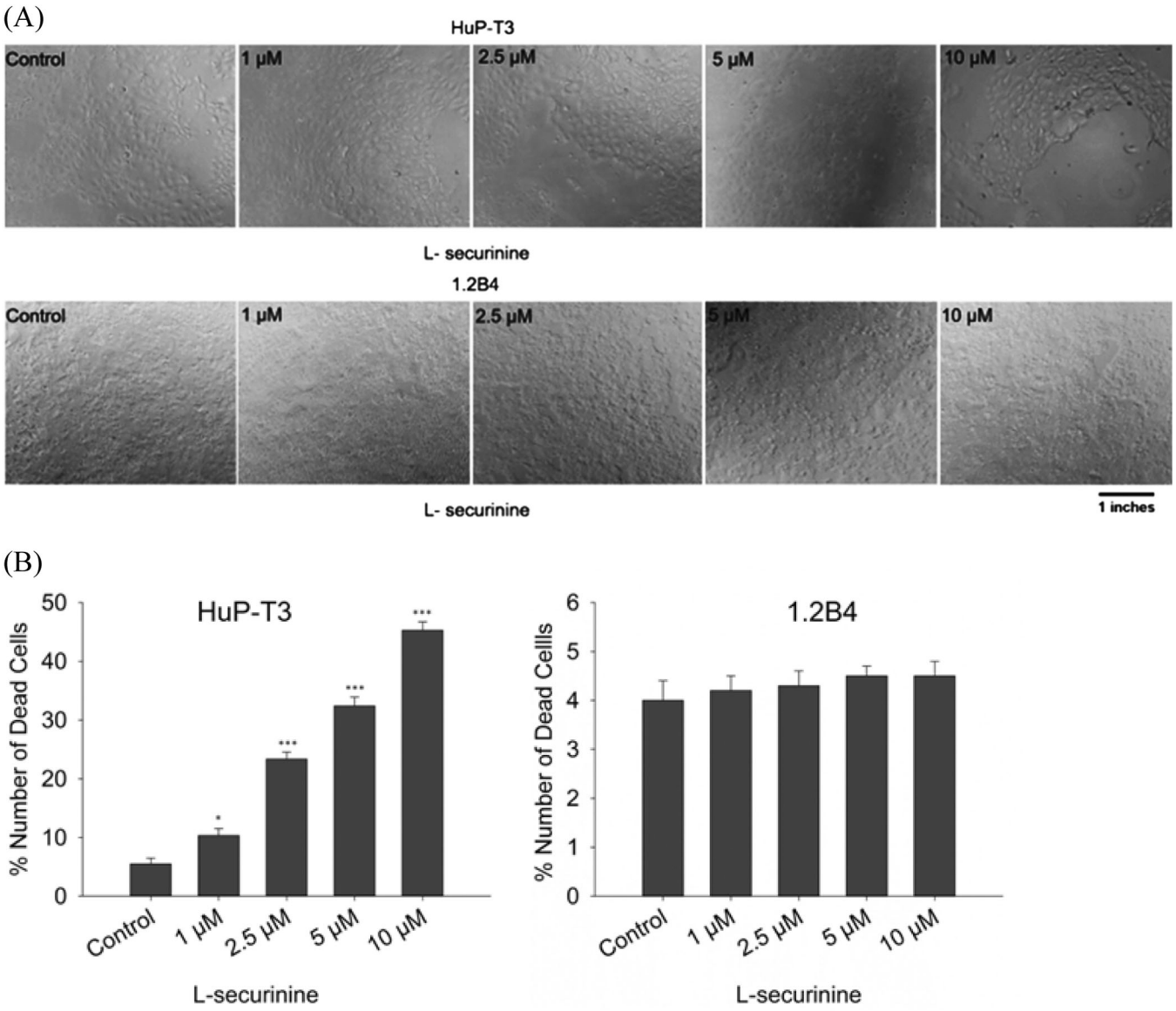

FIGURE 2 | Number of Dead cells of HuP-T3 and 1.2B4. L-securinine inhibits the growth of HuP-T3, whereas no change was observed in cell death levels of 1.2B4. (A) Images were acquired at 10x magnification. Scale bar = 1 inches. Cell death was determined by trypan blue assay. HuP-T3 and 1.2B4 cells were cultured with L-securinine in several concentrations (control = 0.1% v/v vehicle of DMSO, 1, 2.5, 5, and 10 μM) for 24, 48 and 72 h. (B) The data are expressed as mean ± SD of three independent experiments ($N = 3$). Statistical significance was determined by one-way ANOVA followed by the Dunnett's T3 post hoc test; where *p-value < 0.05; **p-value < 0.01; ***p-value < 0.001 in comparison with control group. ANOVA, analysis of variance; DMSO, dimethyl sulfoxide; SD, standard deviation.

25 mg/mL DMSO (25300-062, Thermo Scientific, Fremont, CA, USA) because of its poor water solubility. The final concentration of DMSO in the medium was 0.1% v/v. Before experiments and after treatments with L-securinine, cells were washed twice with phosphate-buffered saline (PBS).

2.2 | 3-(4,5-Dimethylthiazol-2-yl)-2,5-diphenyltetrazolium bromide (MTT) Measurement

In 96-well plates, six biological replicates of HuP-T3 and 1.2B4 were seeded, as described above [15, 16]. The reagent MTT (#30006, Biotium Inc, Landing Parkway Fremont, CA, USA) was added to each well after the treatment. Cells were incubated with MTT for 4 h in the incubator (37°C, 5% humidified CO_2 atmosphere). MTT final concentration was 0.5 mg/mL The MTT assay is based on the cleavage of the yellow tetrazolium salt MTT to purple formazan crystal by metabolic active cells. This purple formazan precipitate was dissolved in DMSO and the color intensity was measured at 570 nm. Measure background absorbance at 630 nm was removed from signal absorbance to obtain normalized absorbance values (optical density (OD)). Cell viability (%) = (experimental group OD − zero adjustment group OD)/(control group OD − zero adjustment group OD) ×

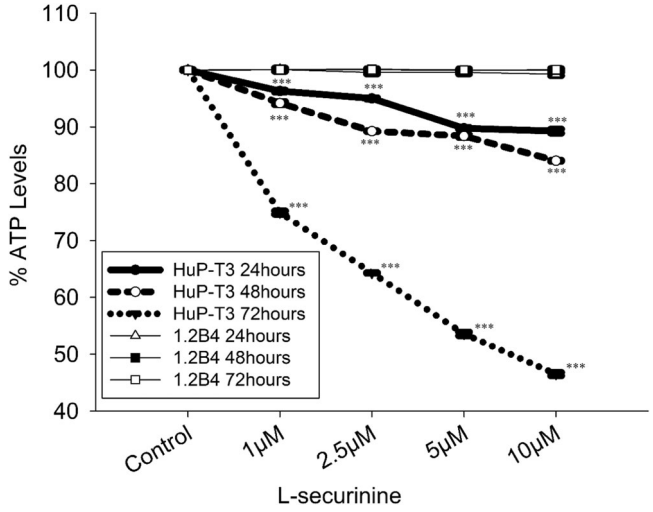

FIGURE 3 | ATP levels of HuP-T3 and 1.2B4. L-securinine inhibits proliferation levels of HuP-T3, whereas no change was observed in proliferation levels of 1.2B4. ATP levels as determined by Vialight Plus assay kit. HuP-T3 and 1.2B4 cells were cultured with L-securinine in several concentrations (control = 0.1% v/v vehicle of DMSO, 1, 2.5, 5, and 10 μM) for 24, 48 and 72 h. The data are expressed as mean ± SD of three independent experiments ($N = 3$). Statistical significance was determined by one-way ANOVA followed by the Dunnett's T3 post hoc test; where **p*-value < 0.05; ***p*-value < 0.01; ****p*-value < 0.001 in comparison with control group. ANOVA, analysis of variance; ATP, adenosine triphosphate; DMSO, dimethyl sulfoxide; SD, standard deviation.

100%. Absorbance measurements were performed with a MultiskanTM FC Microplate Photometer (Thermo Scientific, USA).

2.3 | Cell Counting

In 96-well plates, six biological replicates of HuP-T3 and 1.2B4 were seeded, as described above. Cells photographed at 72 h using phase contrast microscopy at 10× magnification. Cell Counting Kit, 30 dual-chambered slides, 60 counts, with trypan blue (#1450003, Bio-Rad Laboratories, Greece) was used to measure dead cells according to the manufacturer's instructions in a TC20 Automated Cell Counter (Bio-Rad Laboratories, Greece).

2.4 | ATP Measurement

As described above, six biological replicates of the HuP-T3 and 1.2B4 were seeded in 96-well plates. Using an ATP Vialight Plus test kit (LT07-12, Lonza, Switzerland) and an ATP standard (LT27-008, Lonza, Switzerland), the cellular ATP concentrations were measured at the end of the treatment as previously mentioned [15, 16].

2.5 | Immunofluorescence of Ki-67

We used a recombinant anti-Ki67 antibody staining kit (Abcam, Cambridge, UK) according to the manufacturer's instructions. Cells were fixed with paraformaldehyde 4% and permeabilized with Triton x-100 0.25% in PBS. Cells were incubated with primary antibody (1/50 in DPBS) overnight at 4°C. An atto488-conjugated donkey anti-rabbit polyclonal (1/50) was used as the secondary antibody (Sigma-Aldrich, USA). Images of the cells were then taken under a confocal microscope (Olympus Fluoview, FV1000, Hamburg, Germany).

2.6 | Glucose-Induced Insulin Secretion

1.2B4 cells were seeded in 24 well plates. The method used to measure insulin production in response to glucose was reported by Mergelen et al. [17]. The treated cells with L-securinine were first pre-incubated with Krebs-Ringer bicarbonate HEPES buffer, as described by Anastasiou et al. [15]. The insulin enzyme-linked immunosorbent assay (ELISA) kit (EZHI-14K, Sigma-Aldrich, USA) was used to assess insulin levels. Using the BCA Protein Assay Kit (Thermo Scientific, Rockford, IL, USA), the protein content was measured and used to standardize the levels of insulin secretion. Thermo Scientific, USA's MultiskanTM FC Microplate Photometer was used to detect absorbance at 450 nm.

2.7 | Detection of Cell Apoptosis

HuP-T3 and 1.2B4 cells were seeded in 6-well plates in biological [15, 16, 18]. Then cells were resuspended in 500 μL PBS and added 4.5 mL frozen ethanol (80%). Cells were incubated at 4°C for 20 min. After that, cells were centrifuged at 200*g* for 5 min at 4°C and the supernatants were removed. Then cells were washed with cold PBS, centrifuged at 200*g* for 5 min and the supernatant was removed. 0.1% Triton X-100 was added for 5 min, the cells were centrifuged for 5 min and the supernatant was removed, while they were washed again as described above. Finally, the cells were resuspended in 100 μL propidium iodide (PI) staining solution (including Tris-HCl pH 7.5 100 mM, NaCl 150 mM, $Cacl_2$ 1 mM, $Mgcl_2$ 0.5 mM, NP-40 0.1% PI [4 μg/mL] and ribonuclease [0.1 mg/mL]) and incubated for 30 min at room temperature protected from the light [19] After the incubation, 400 μL PBS was added and cell cycle analysis was estimated on a flow cytometer (BD FACSCalibur - BD Biosciences, San Jose, CA, USA) in the FL2 channel. Positive cells (PI)/total cells × 100% represented the percentage of PI-positive cells.

2.8 | Determination of Intracellular ROS

We Intracellular ROS was detected using a 2′,7′-dichlorofuorescein diacetate (DCFDA) (ab113851, Abcam, Cambridge, MA, USA) assay kit according to the manufacturer protocol. Here, HuP-T3 cells were grown on eight-chamber slides in biological triplicates. Once cells reached a confluence of 70%, they were treated with L-securinine for 72 h, as described above. Then, cells were washed twice with PBS and then incubated with 25 μM DCFDA in an essential medium with 10% FBS in the incubator (37°C, 5% humidified CO_2 atmosphere) for 30 min. Images of the cells were

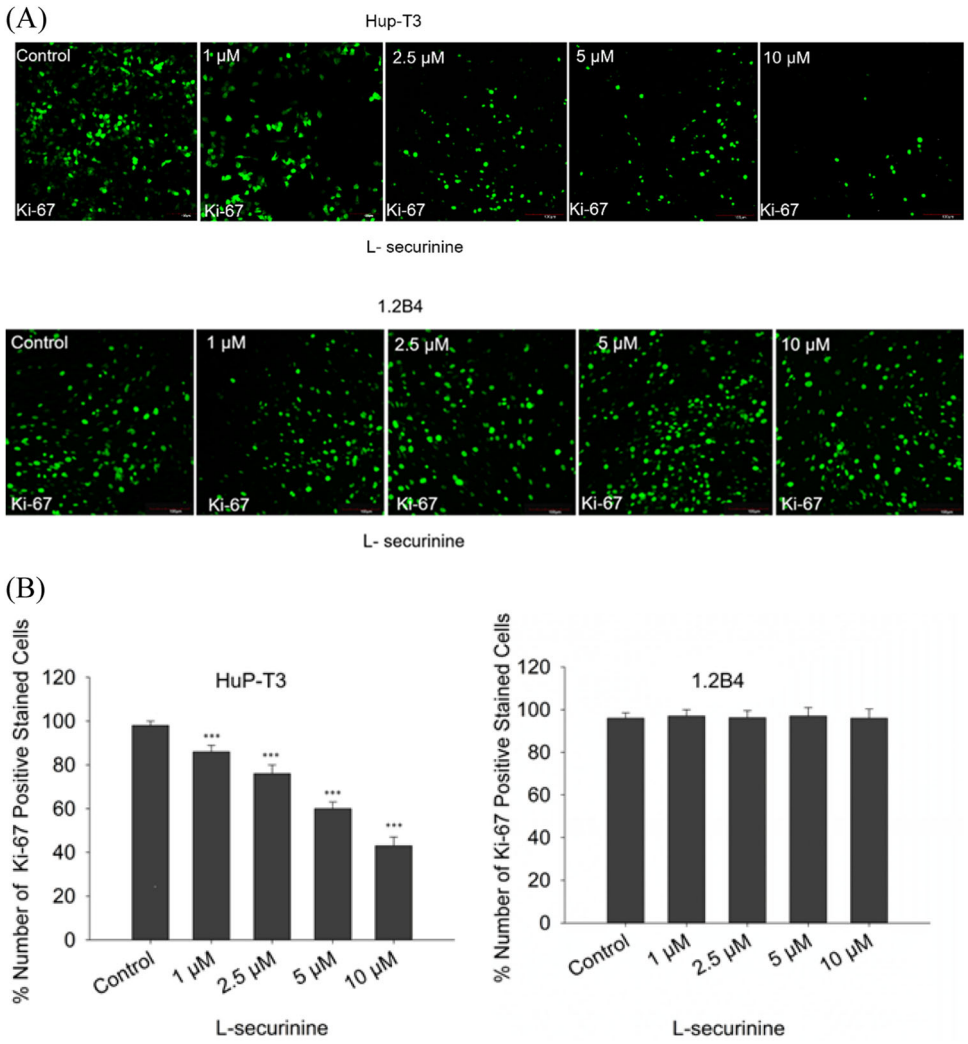

FIGURE 4 | Number of Ki-67 positive stained cells of HuP-T3 and 1.2B4. L-securinine inhibits the proliferation of HuP-T3. (A) Cell proliferation was determined by immunofluorescence of Ki-67. HuP-T3 and 1.2B4 cells were cultured with L-securinine in several concentrations (control = 0.1% v/v vehicle of DMSO, 1, 2.5, 5, and 10 μM) for 72 h. (A) Images were acquired at 10x magnification. Scale bar = 100 μm (B) The data are expressed as mean ± SD of three independent experiments ($N = 3$). Statistical significance was determined by one-way ANOVA followed by Dunnett's T3 post hoc test; where **p*-value < 0.05; ***p*-value < 0.01; ****p*-value < 0.001 in comparison with the control group. ANOVA, analysis of variance; DMSO, dimethyl sulfoxide; SD, standard deviation.

then taken under a confocal microscope (Olympus Fluoview, FV1000, Hamburg, Germany) [15].

2.9 | RNA Preparation and Quantitative Real-Time Polymerase Chain Reaction (RT-qPCR)

The Nucleospin RNA Plus kit (740984.250, Macherey–Nagel, Germany) was used to extract total RNA (500 ng) from a six-well plate according to the manufacturer's instructions and as described before. [16] Supporting Information: Table 1 shows the target genes with their characteristics along with the primer pairs. Primers were designed as described before [20]. The comparative Ct ($2^{-\Delta\Delta Ct}$) method was used to determine the relative gene expression levels [20], while the normalization was based on actin beta (ACTB). ACTB was selected because its levels of expression were unaffected by a variety of biological interventions [21].

2.10 | Western Blot Analysis

HuP-T3 and 1.2B4 cells were seeded in dishes 100 mm as described above [15]. Trypsin/EDTA was then used to quickly harvest the cells. After thoroughly rinsing the cells with PBS, the cells were centrifuged for 10 min at 4°C at 200*g*. Next, the cells were lysed in an ice-cold radio-immunoprecipitation assay lysis buffer for 1 h. This buffer contained 50 mM Tris-HCl pH 7.4, 150 mM NaCl, 0.1% sodium dodecyl sulfate (SDS), 1 mM EDTA, 1% Triton X-100, 1 mM phenylmethylsulfonyl fluoride, 1:100 protease inhibitor, 1:100 phosphatase inhibitor, and 1 mM phenylmethylsulfonyl fluoride. After the lysates were collected, they were centrifuged for 10 min at 4°C at 20,000*g*. The Bradford protein assay was used to determine the total protein concentrations after the supernatants were moved to a new tube. Cell Signaling Technology (Danvers, MA, USA) is the source of all antibodies, biotinylated protein ladder (7727, dilution 1:1000), nitrocellulose membranes (12369),

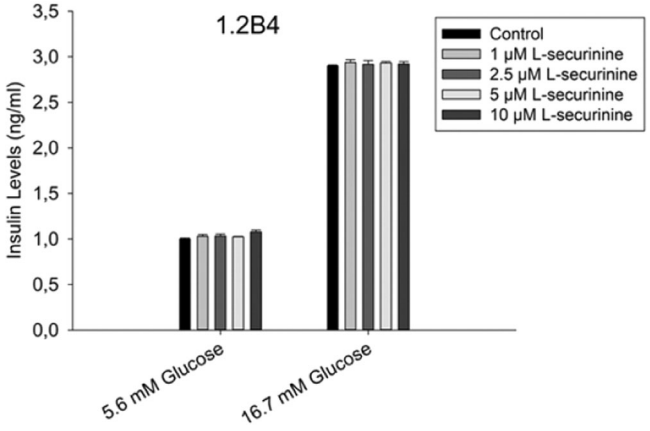

FIGURE 5 | Insulin secretion levels (ng/ml). 1.2B4 cells were cultured with L-securinine in several concentrations (control = 0.1% v/v vehicle of DMSO, 1, 2.5, 5, and 10 μM) for 72 h. The bar diagram represents the quantitative data. The data is presented as mean ± SD of three independent experiments ($N = 3$). Statistical significance was determined by one-way ANOVA followed by the Dunnett's T3 post hoc test; where *p-value < 0.05; **p-value < 0.01; ***p-value < 0.001 in comparison with the control group. ANOVA, analysis of variance; DMSO, dimethyl sulfoxide; SD, standard deviation.

20X lumiGLO reagent, and 20X peroxide (95538S). For western blot analysis, equal amounts of protein (40 μg) and ladder were separated by a gradient 7.5%–12% SDS polyacrylamide gel and transferred onto nitrocellulose membranes. The immunoblot membranes were incubated with a blocking solution consisting of 5% milk or bovine serum albumin in Tris-Buffered Saline 0.1% Tween for 1 h at room temperature and then incubated at 4°C on a shaker overnight with the primary antibodies. The next day, the primary antibodies were removed, and the membranes were incubated with secondary antibodies (anti-rabbit IgG and anti-mouse IgG) at 37°C for 1 h (loading controls, primary, and secondary antibodies detailed in Supporting Information: Table 2). Antibody-binding bands were visualized with 20X lumiGLO reagent and 20X Peroxide (dilution 1:20). The density of the bands was quantified with Image Pro Plus version 6.0 software (Media Cybernetics, Maryland, MD, USA) and normalized against loading control (β-Actin). Primary and secondary antibodies are detailed in Supporting Information: Table 2. The phosphorylated forms of akt were normalized against total akt.

2.11 | Statistics and Graph Presentation

The statistical packages SigmaPlot 12.2 (Systat Software Inc., San Jose, CA, USA) and IBM SPSS Statistics for Windows, Version 23.0, IBM Corp., Armonk, NY, USA, were used for the analyses. All data were assessed for normal distribution of their values with the use of the Shapiro–Wilk test. Normally distributed variables are presented as means ± standard deviation (SD). Differences across study groups were compared using one-way analysis of variance (ANOVA), and additional analysis of the data was performed using Dunnett's T3 post hoc test. Should the p-value be less than 0.05, the comparison was deemed statistically significant.

3 | Results

3.1 | L-Securinine Reduces the Viability of Pancreatic Adenocarcinoma Cells

To determine the viability of pancreatic cells after the application of L-securinine, two pancreatic cell lines (HuP-T3, a cancer cell line, and 1.2B4, a hybrid cell line) were treated with varying concentrations of L-securinine (1, 2.5, 5, and 10 μM) for different time intervals (24, 48, and 72 h). An MTT assay was performed to measure the cells' growth. As demonstrated in Figure 1, treatment with 1, 2.5, 5, and 10 μM of L-securinine for 24 and 48 h resulted in an inhibitory effect on the cell viability of HuP-T3 cells in comparison with the control group. Of note, the differences in the viability levels between all treatment groups (1, 2.5, 5, and 10 μM) and the control group were larger at the 72-h point. On HuP-T3 cells the IC50 was 8.25 μM at 72-h point. Importantly, no significant inhibitory effect of L-securinine was observed on 1.2B4 cells after 24, 48, and 72 h of exposure to any concentration ($p > 0.05$). Therefore, L-securinine is cytotoxic for HuP-T3 cells; however, it does not exhibit cytotoxicity towards 1.2B4 cells.

3.2 | L-Securinine Increases the Number of Death in Pancreatic Adenocarcinoma Cells

To determine the number of dead pancreatic cells after the application of L-securinine, two pancreatic cell lines (HuP-T3, a cancer cell line, and 1.2B4, a hybrid cell line) were treated with varying concentrations of L-securinine (1, 2.5, 5, and 10 μM) for 72 h. A cell counting assay was performed to measure the cells' death. As demonstrated in Figure 2, treatment with 1, 2.5, 5, and 10 μM resulted in an increase on the cells death of HuP-T3 cells in comparison with the control group. Importantly, no significant inhibitory effect of L-securinine was observed on 1.2B4 cells after 72 h of exposure to any concentration ($p > 0.05$). Therefore, L-securinine is cytotoxic for HuP-T3 cells; however, it does not exhibit cytotoxicity towards 1.2B4 cells.

3.3 | L-Securinine Reduces the Atp Levels of Pancreatic Adenocarcinoma Cells

To determine the proliferation rate of L-securinine on pancreatic cells, two cell lines, Hup-T3 and 1.2B4, were treated with varying concentrations of L-securinine (1, 2.5, 5, and 10 μM) for different time intervals (24, 48, and 72 h). An ATP assay was performed to quantify the cells' proliferation rate. As demonstrated in Figure 3, treatment with 1, 2.5, 5, and 10 μM of L-securinine for 24 and 48 h resulted in an inhibitory effect on the proliferation rate of HuP-T3 cells in comparison with the control group. Of note, there were significant differences in the proliferation rate between all treatment groups (1, 2.5, 5, and 10 μM) and the control group at the 72-h point for HuP-T3 cells. In contrast, no significant inhibition of proliferation was observed on 1.2B4 cells after exposure to any concentration of L-securinine for 24, 48, and 72 h ($p > 0.05$). Therefore, L-securinine selectively inhibits the proliferation rate only for HuP-T3 cells.

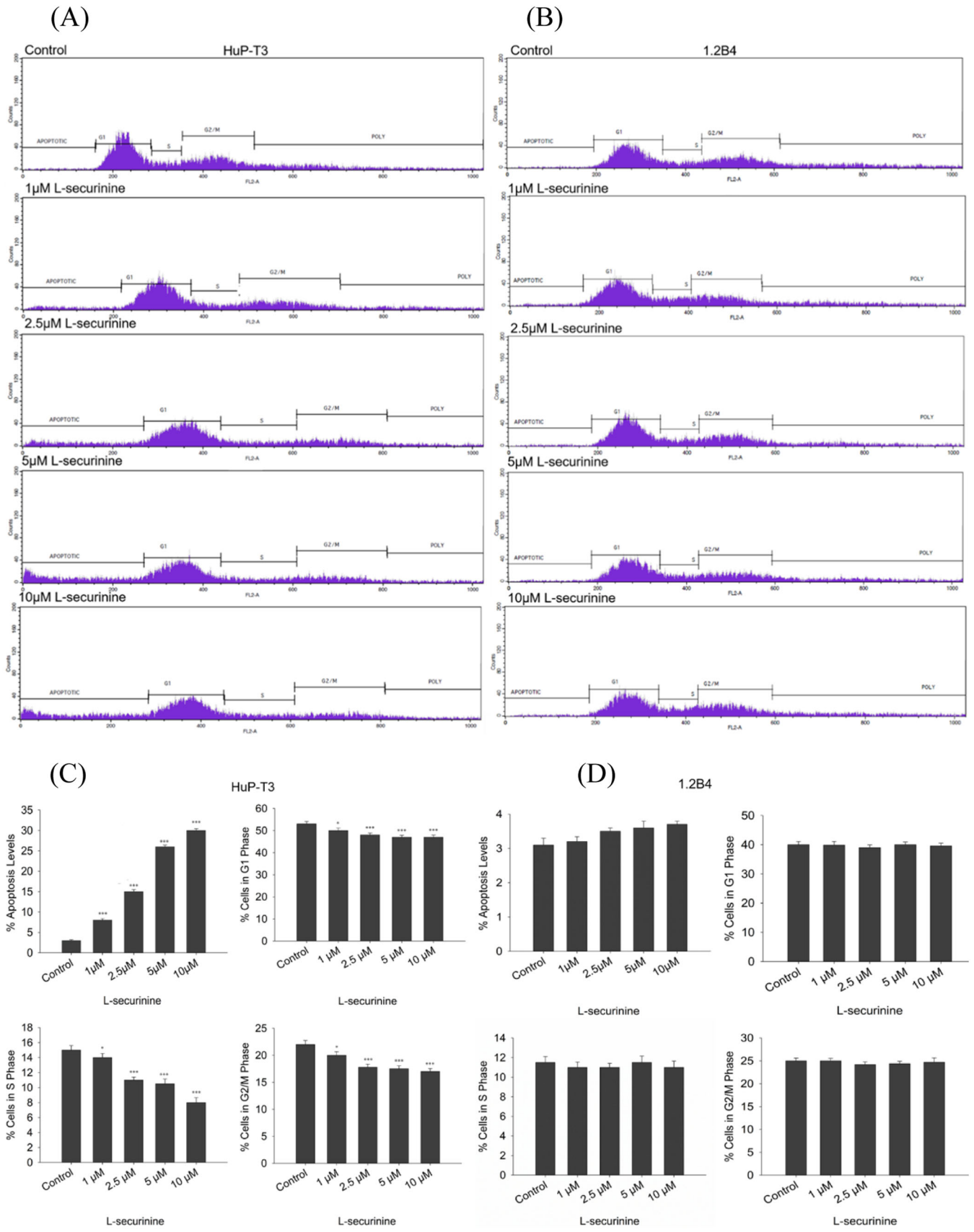

FIGURE 6 | Legend on next page.

3.4 | L-Securinine Inhibits the Proliferation of Pancreatic Adenocarcinoma Cells

To determine the proliferation rate of L-securinine on pancreatic cells, two cell lines, Hup-T3 and 1.2B4, were treated with varying concentrations of L-securinine (1, 2.5, 5, and 10 μM) for 72 h. An immunofluorescence expression of Ki-67 was performed to quantify the cells' proliferation rate. As demonstrated in Figure 4, treatment with 1, 2.5, 5, and 10 μM of L-securinine for 72 h resulted in an inhibitory effect on the proliferation rate of HuP-T3 cells in comparison with the control group. In contrast, no significant inhibition of proliferation was observed on 1.2B4 cells after exposure to any concentration of L-securinine for 72 h ($p > 0.05$). Therefore, L-securinine selectively inhibits the proliferation rate only for HuP-T3 cells.

3.5 | L-Securinine Did Not Affect the Insulin Levels or Content of 1.2B4 Cells

To further validate the hybrid β-cell function of 1.2B4 cells after treatment with L-securinine, insulin levels and content were assessed. To elucidate insulin secretion, 1.2B4 cells were incubated for 72 h with varying concentrations of L-securinine (1, 2.5, 5, and 10 μM) in response to low (5.6 mM) and high (16.7 mM) concentrations of glucose. Incubating cells with L-securinine for 72 h did not significantly alter insulin secretion at 5.6 mM and 16.7 mM glucose as compared to the control group (Figure 5). Also, L-securinine did not affect the insulin levels and content of 1.2B4 cells.

3.6 | L-Securinine Induces the Apoptosis of Pancreatic Adenocarcinoma Cells

As demonstrated in Figure 6A, cells were labeled with PI and subjected to flow cytometry analysis further to confirm apoptosis and cell cycle levels at 72 h, when we identified the more substantial inhibitory impact of HuP-T3 treated with L-securinine. The results in Figure 6C show a significantly higher proportion of apoptotic HuP-T3 cells after incubation with 1, 2.5, 5, and 10 μM concentrations of L-securinine in comparison with the control group. After incubation with varying concentrations of L-securinine (1, 2.5, 5, and 10 μM), the levels of G1, S, and G2/M phases decreased compared to the control group. These results suggest that L-securinine effectively promoted apoptosis of HuP-T3 cells in a dose–dependent manner. In contrast, no significant change was observed on 1.2B4 cells after exposure to any concentration of L-securinine as shown in Figures 6B,D.

3.7 | L-Securinine Increases Intracellular ROS Production in Pancreatic Adenocarcinoma Cells

In an attempt to determine the precise apoptotic mechanism L-securinine triggers, we investigated intracellular ROS production. The DCFH-DA fluorescent dye was applied to estimate the generation of intracellular ROS on HuP-T3 and 1.2B4. As shown in Figure 7A, treatment for 72 h with L-securinine boosted intracellular ROS generation on HuP-T3 cells. In Figure 7B, it is evident that at all concentrations of L-securinine (1, 2.5, 5, and 10 μM), ROS activation and production increased compared to the control group. In contrast, no significant generation of intracellular ROS was observed on 1.2B4 cells after exposure to any concentration of L-securinine for 72 h ($p > 0.05$) data not shown.

3.8 | L-Securinine Regulates the Expression of Cancer Apoptosis-Associated Genes

To gain more insight into the mechanism by which L-securinine causes apoptosis in HuP-T3 cells, RT-qPCR experiments were employed to quantify the relative expression levels of genes linked to apoptosis, including cleaved caspase-3, cleaved caspase-9, Bax, and Bcl-2.

As shown in Figure 8 A, after treatment with L-securinine (1, 2.5, 5, and 10 μM), it was found that the expression of proapoptotic Bax protein was increased. In contrast, the expression of the antiapoptotic Bcl-2 protein appeared to be markedly decreased in a dose-dependent manner on HuP-T3 cells. These differences were statistically significant compared with the control group. Moreover, following L-securinine treatment, there was a significant increase in cleaved caspase-9, and cleaved caspase-3 was detectable on HuP-T3 cells. Subsequently, poly-(ADP-ribose)-polymerase-1 (PARP-1), a known substrate of caspase-3, underwent cleavage. Hence, these data indicate that L-securinine induces apoptosis on HuP-T3 cells. Then, the PI3K/AKT/mTOR/PTEN pathway gene expression was measured by quantitative real-time RT-PCR. The PI3K/AKT/mTOR/PTEN signaling pathway, crucial for cell growth and proliferation, is implicated in the mechanism of L-securinine-induced apoptosis on HuP-T3 cells. Specifically, L-securinine treatment led to the downregulation of PI3K, AKT, and mTOR gene expression and the upregulation of PTEN gene expression on HuP-T3 cells in a dose-dependent manner. In contrast, no significant change was found on genes expression levels after exposure of 1.2B4 cells to any concentration of L-securinine (Figure 8B). Supporting Information: Tables 3 and 4 show values and R2 of all the genes.

FIGURE 6 | Apoptosis and cell cycle levels on L-securinine treated HuP-T3 and 1.2B4. (A), (B) Dot-plot represents levels of apoptosis and cell cycle. Apoptosis and cell cycle levels was detected by flow cytometry using PI staining. (C), (D), The bar diagram represents the quantitative data. HuP-T3 and 1.2B4 cells were cultured with L-securinine in several concentrations (control = 0.1% v/v vehicle of DMSO, 1, 2.5, 5, and 10 μM) for 72 h. The data is presented as mean ± SD of three independent experiments ($N = 3$). Statistical significance was determined by one-way ANOVA followed by Dunnett's T3 post hoc test; where *p-value < 0.05; **p-value < 0.01; ***p-value < 0.001 in comparison with the control group. ANOVA, analysis of variance; DMSO, dimethyl sulfoxide; PI, propidium iodide; SD, standard deviation.

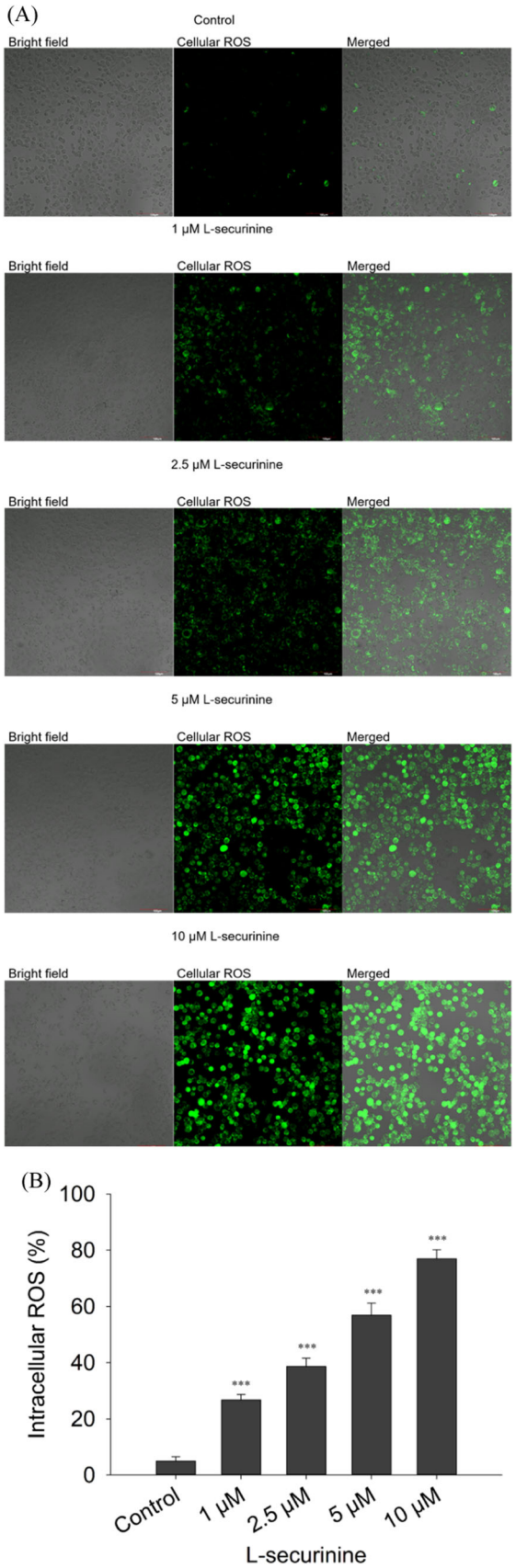

3.9 | L-Securinine Regulates the Expression of Cancer Apoptosis-Associated Proteins

To examine in detail the role of the L-securinine in apoptosis pathway on HuP-T3 we used western blot analysis to study the expression of signaling molecules and apoptotic proteins. Phosphorylated form of Akt, mTOR, cleaved caspase-9, and cleaved caspase-3 were quantified. As shown in Figure 9 L-securinine decreased significantly the expression of phosphorylated form of Akt, mTOR and increased the expression levels of the apoptotic proteins' caspase-9 and caspase-3 in a dose-dependent way in comparison with the control group. In contrast, no significant protein expression was observed on 1.2B4 cells after exposure to any concentration of L-securinine.

4 | Discussion

Identifying novel natural compounds mediating cancer cell cytotoxicity with high specificity and low nonspecific toxicity is a valuable strategy for developing antitumor drugs [22]. Herein, we investigated the effect of L-securinine on the viability and proliferation levels of HuP-T3 and 1.2B4 cells for up to 72 h. Our results demonstrated that L-securinine inhibited both proliferation and growth of Hup-T3 cells, showing inhibitory and antiproliferative activity in comparison with the control group. However, L-securinine had no impact on the proliferation and growth of 1.2B4 cells, nor on their insulin levels and content.

Antineoplastic medications use a variety of methods to kill tumor cells. They frequently trigger apoptosis or programmed cell death [23]. In the present study, flow cytometry analysis revealed that the rate of apoptosis in L-securinine-treated HuP-T3 cells was increased in a dose-dependent manner at 72 h. The presence of numerous active oncogenic signaling pathways, such as PI3K/Akt/mTOR, which increases treatment resistance and disease aggressiveness, is another important characteristic of pancreatic cancer. Since L-securinine affects this pathway, it justifies this selective effectiveness. On the contrary, L-securinine had no impact on apoptosis and cell cycle levels of 1.2B4 cells. Additionally, we observed an elevation in intracellular ROS levels on HuP-T3 cells after exposure to L-securinine. We also analyzed the impact of L-securinine on

FIGURE 7 | L-securinine increased cellular reactive oxygen species (ROS) production. Intracellular ROS were assessed by DCFDA. Hup-T3 cells were cultured with L-securinine in several concentrations (control = 0.1% v/v vehicle of DMSO, 1, 2.5, 5, and 10 μM) for 72 h. ROS generation was detected in the green fluorescent channel. (A) Images in the left column show Hup-T3 on bright field the images in the middle column show the production of ROS (green); images in the right column show overlay of ROS with bright field. Images were acquired at 20x magnification. Scale bar = 100 μm. (B) The bar diagram represents the quantitative data. The data is presented as mean ± SD of three independent experiments ($N = 3$). Statistical significance was determined by one-way ANOVA followed by Dunnett's T3 post hoc test; where *p-value < 0.05; **p-value < 0.01; ***p-value < 0.001 in comparison with the control group. ANOVA, analysis of variance; SD, standard deviation.

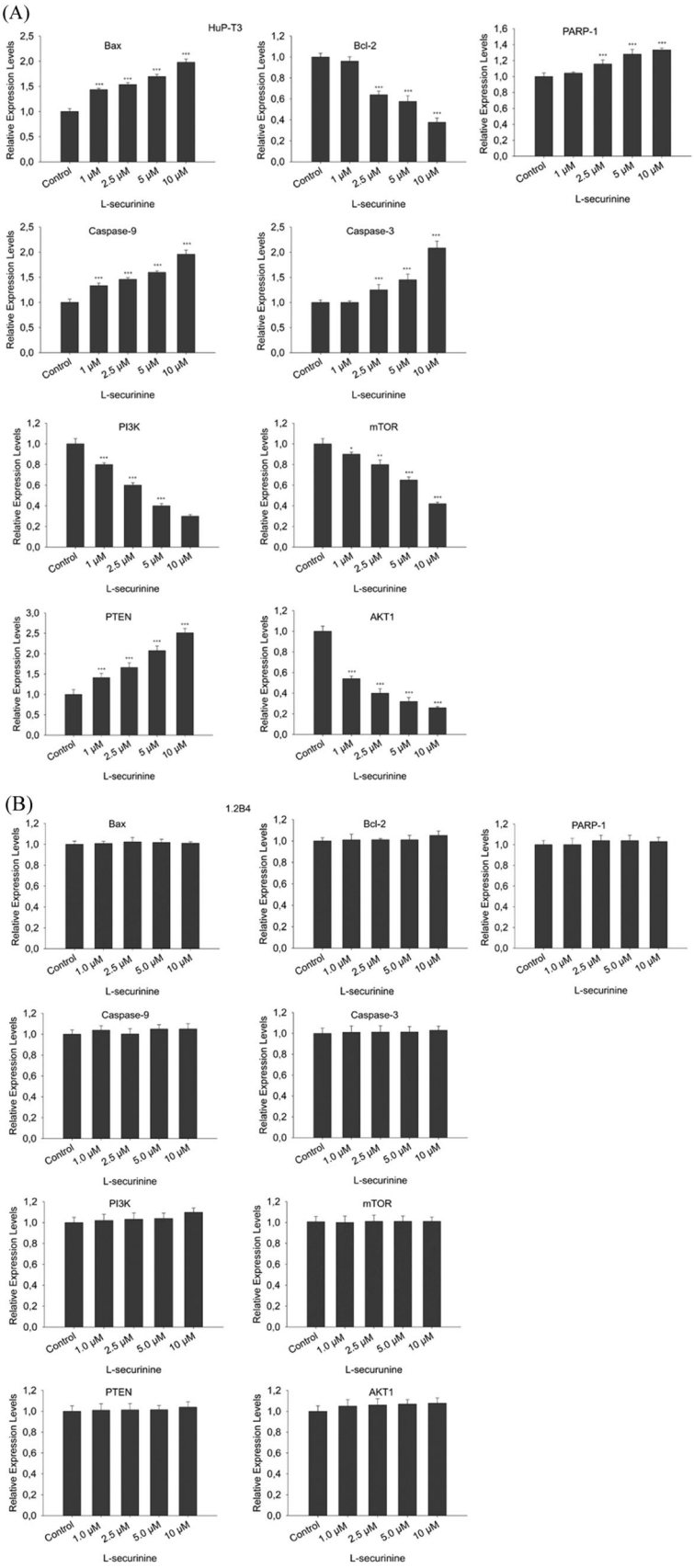

FIGURE 8 | (A), (B) Relative expression levels of Bax, Bcl-2, cleaved caspase-9, cleaved caspase-3, PI3K, mTOR, AKT1, PTEN, and PARP on HuP-T3 and 1.2B4. The ACTB was used as internal reference gene. The data are expressed as mean ± SD of three independent experiments ($N = 3$). Statistical significance was determined by one-way ANOVA followed by Dunnett's T3 post hoc test; where *p-value < 0.05; **p-value < 0.01; ***p-value < 0.001 in comparison with control group. ACTB, actin beta; ANOVA, analysis of variance; SD, standard deviation.

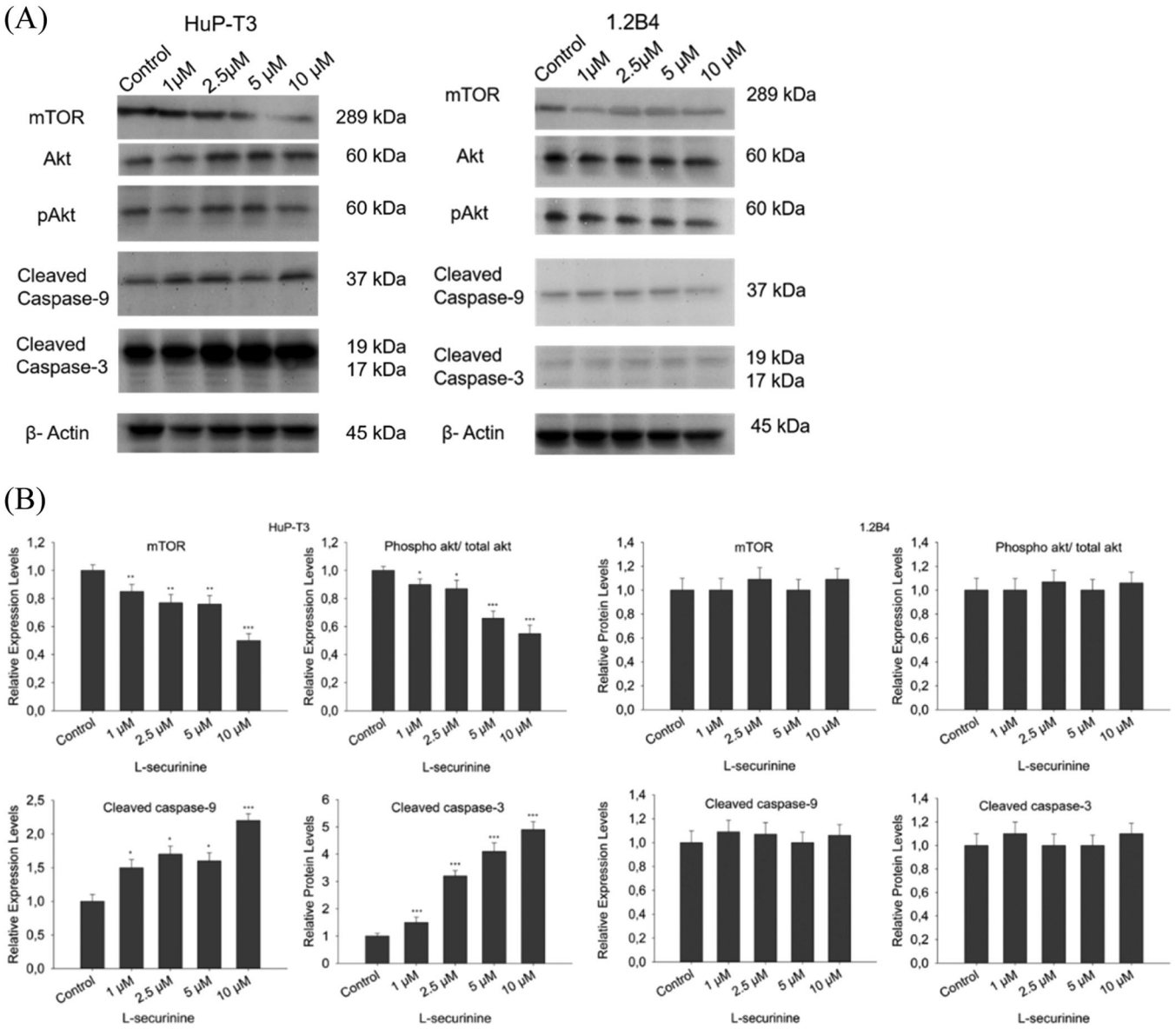

FIGURE 9 | (A) Western blot analysis of mTOR, phospho Akt, cleaved caspase-9, cleaved caspase-3, on HuP-T3 and 1.2B4. β-Actin is the loading Control. (B) The bar diagram represents the quantitative data. The data is presented as mean ± SD of three independent experiments ($N = 3$). Statistical significance was determined by one-way ANOVA followed by Dunnett's T3 post hoc test; where *p-value < 0.05; **p-value < 0.01; ***p-value < 0.001 in comparison with the control group. ACTB, actin beta; ANOVA, analysis of variance; SD, standard deviation.

mRNA expression levels of key genes (Bax, Bcl-2, cleaved caspase-9, cleaved caspase-3, and PARP-1) on HuP-T3 cells over 72 h. Our qRT-PCR results revealed that L-securinine upregulated the RNA level of the proapoptotic Bax, leading to apoptosis on HuP-T3 cells. Conversely, the antiapoptotic gene *bcl-2* showed downregulated expression. Bax and Bcl-2, both crucial members of the Bcl-2 family, play pivotal roles in cellular fate [24]. Bcl-2 acts as an antiapoptotic signal, while Bax serves as a proapoptotic signal and is less expressed in many human cancers [25]. Their dysregulation is associated with chemotherapeutic drug resistance in various human cancers [26]. Moreover, we observed a significant increase in relative expression levels of cleaved caspase-9, cleaved caspase-3, and PARP-1 on HuP-T3. The final molecule of apoptosis, the effector caspase-3, is eventually activated by cleaved caspase-9 [27]. We also confirmed these data with the relative protein levels of cleaved caspase-9 and the effector cleaved caspase-3, the final molecule of apoptosis.

The PI3K/AKT/mTOR signaling pathway is considered the "survival pathway" for its essential role in cell differentiation, proliferation, and survival [28]. Therefore, the PI3K/AKT/mTOR pathway is an appealing target, and the inhibition of this pathway holds promise as an effective therapy for cancer [29]. The present study revealed that L-securinine treatment affected the expression of genes involved in the PI3K/AKT/mTOR signaling pathway on HuP-T3 at 72 h. L-securinine administration specifically resulted in dose-dependent downregulation of PI3K, AKT, and mTOR relative expression levels and upregulation of PTEN gene expression. We also confirmed that L-securinine decreased the expression of the relative protein levels of mTOR and the phosphorylated form of Akt, in a dose-dependent

manner. These findings suggest that pancreatic adenocarcinoma treatment strategies may be developed by focusing on the PI3K/AKT/mTOR signaling pathway. When combined, our findings show that PI3K/AKT/mTOR signaling plays a novel and crucial role in the process via which L-securinine causes HuP-T3 cells to undergo ROS-dependent apoptosis. Many antineoplastic drugs exercise their antitumor effects on cancer cells by inducing apoptosis, offering several signals for successful anticancer treatment [30, 31]. Our results showed that the apoptotic index of Hup-T3 cells increased in a dose-dependent manner. These findings strongly support the development of L-securinine as a promising antineoplastic agent for clinical applications. Multiple studies suggest that the pancreatic adenocarcinoma microenvironment boosts tumor growth, promotes metastasis and creates a physical barrier to drug delivery. Combination treatments have a lot of potential to improve immune responses and provide better therapeutic outcomes [30–32].

In our study, we used one major pancreatic carcinoma model (Hup-T3) to determine the effect of L-securinine on cancer cells and the hybrid 1.2B4 cell line as contol. The inhibitory effect of L-securinine has been demonstrated in other cancers, but not on pancreatic cancer cells. Our results focus on the in vitro effects of L-securinine and is the first step in studying its activity against pancreatic cancer. Our study covers a gap in the literature, although more studies are needed on the topic. These data highlight L-securinine's potential as an anticancer agent, although additional research is needed to evaluate its effects in animal models and eventually in human clinical trials.

5 | Conclusions

In summary, our study demonstrates that L-securinine triggers ROS-dependent apoptosis on pancreatic cancer cells while inhibiting the PI3K/AKT/mTOR signaling pathway. These findings suggest that L-securinine holds promise as a potential lead for future drug development in the fight against pancreatic adenocarcinoma.

Author Contributions

Ioanna A. Anastasiou: conceptualization, investigation, funding acquisition, writing–original draft, methodology, validation, visualization, writing–review and editing, software, formal analysis, project administration, data curation, resources. **Panagiotis Sarantis:** visualization, formal analysis, project administration. **Eleni Rebelos:** visualization, project administration. **Ioanna Eleftheriadou:** formal analysis. **Konstantinos N. Tentolouris:** formal analysis, supervision. **Athanasia Katsaouni:** supervision. **Evangelos Koustas:** visualization. **Vasileia Kokala:** supervision. **Michalis V Karamouzis:** supervision. **Nikolaos Tentolouris:** supervision, funding acquisition.

Acknowledgments

The research, writing, and/or publishing of this work were made possible by the following financial assistance granted to the authors: The research was supported by National and Kapodistrian University of Athens, Greece's Special Account for Research Grants (SARG) (SARG 70/3/16125).

Conflicts of Interest

The authors declare no conflicts of interest.

Data Availability Statement

The data that support the findings of this study are available from the corresponding author upon reasonable request.

References

1. E. Sarfaty, N. Khajoueinejad, M. G. Zewde, A. T. Yu, and N. A. Cohen, "Surgical Management of Pancreatic Ductal Adenocarcinoma: A Narrative Review," *Translational Gastroenterology and Hepatology* 8 (2023): 39.

2. M. A. Duggan, W. F. Anderson, S. Altekruse, L. Penberthy, and M. E. Sherman, "The Surveillance, Epidemiology, and End Results (SEER) Program and Pathology: Toward Strengthening the Critical Relationship," *American Journal of Surgical Pathology* 40, no. 12 (2016): e94–e102.

3. R. L. Siegel, K. D. Miller, N. S. Wagle, and A. Jemal, "Cancer Statistics, 2023," *CA: A Cancer Journal for Clinicians* 73, no. 1 (2023): 17–48.

4. X. Zhang, L.-X. Chen, L. Ouyang, Y. Cheng, and B. Liu, "Plant Natural Compounds: Targeting Pathways of Autophagy As Anti-Cancer Therapeutic Agents," *Cell Proliferation* 45, no. 5 (2012): 466–476.

5. Y. Xia, C. Cheng, S. Yao, Q. Zhang, Y. Wang, and Z. Ji, "L-Securinine Induced the Human Colon Cancer SW480 Cell Autophagy and Its Molecular Mechanism," *Fitoterapia* 82, no. 8 (2011): 1258–1264.

6. D. Raj and M. Łuczkiewicz, "Securinega Suffruticosa," *Fitoterapia* 79 (2008): 419–427.

7. S. Klochkov and M. Neganova, "Unique Indolizidine Alkaloid Securinine Is a Promising Scaffold for the Development of Neuroprotective and Antitumor Drugs," *RSC Advances* 11, no. 31 (2021): 19185–19195.

8. S. Han, G. Zhang, M. Li, et al., "L-Securinine Induces Apoptosis in the Human Promyelocytic Leukemia Cell Line HL-60 and Influences the Expression of Genes Involved in the PI3K/AKT/mTOR Signaling Pathway," *Oncology Reports* 31, no. 5 (2014): 2245–2251.

9. S. M. Ashraf, S. Mahanty, and K. Rathinasamy, "Securinine Induces Mitotic Block in Cancer Cells by Binding to Tubulin and Inhibiting Microtubule Assembly: A Possible Mechanistic Basis for Its Anticancer Activity," *Life Sciences* 287 (2021): 120105.

10. C.-J. Liu, X.-D. Fan, J.-G. Jiang, Q.-X. Chen, and W. Zhu. *Phytomedicine* 106 (2022): 154417.

11. S. Mehra, N. Deshpande, and N. Nagathihalli, "Targeting PI3K Pathway in Pancreatic Ductal Adenocarcinoma: Rationale and Progress," *Cancers* 13, no. 17 (2021): 4434.

12. A. Glaviano, A. S. C. Foo, H. Y. Lam, et al., "PI3K/AKT/mTOR Signaling Transduction Pathway and Targeted Therapies in Cancer," *Molecular Cancer* 22, no. 1 (2023): 138.

13. P. G. Adamopoulos, C. K. Kontos, and A. Scorilas, "Molecular Cloning of Novel Transcripts of Human Kallikrein-Related Peptidases 5, 6, 7, 8 and 9 (KLK5 – KLK9), Using Next-Generation Sequencing," *Scientific Reports* 7, no. 1 (2017): 17299.

14. S. Han, X. Yang, Y. Pan, et al., "L-Securinine Inhibits the Proliferation of A549 Lung Cancer Cells and Promotes DKK1 Promoter Methylation," *Oncology Letters* 14, no. 4 (2017): 4243–4248.

15. I. A. Anastasiou, I. Eleftheriadou, A. Tentolouris, et al., "Low Concentrations of Bisphenol A Promote the Activation of the Mitochondrial Apoptotic Pathway on Beta-TC-6 Cells via the Generation of Intracellular Reactive Oxygen Species and Mitochondrial Superoxide," *Journal of Biochemical and Molecular Toxicology* 36, no. 8 (2022): e23099.

16. I. A. Anastasiou, P. Sarantis, I. Eleftheriadou, et al., "Effects of Hypericin on Cultured Primary Normal Human Dermal Fibroblasts Under Increased Oxidative Stress," *The International Journal of Lower Extremity Wounds* 204 (2023): 291–299.

17. A. Merglen, S. Theander, B. Rubi, G. Chaffard, C. B. Wollheim, and P. Maechler, "Glucose Sensitivity and Metabolism-Secretion Coupling Studied during Two-Year Continuous Culture in INS-1E Insulinoma Cells," *Endocrinology* 145, no. 2 (2004): 667–678.

18. A. M. Rieger, K. L. Nelson, J. D. Konowalchuk, and D. R. Barreda, "Modified Annexin V/Propidium Iodide Apoptosis Assay for Accurate Assessment of Cell Death," *Journal of Visualized Experiments* 50 (2011): 2597.

19. C. Riccardi and I. Nicoletti, "Analysis of Apoptosis By Propidium Iodide Staining and Flow Cytometry," *Nature Protocols* 1, no. 3 (2006): 1458–1461.

20. K. Li and A. Brownley, "Primer Design for RT-PCR," *Methods in Molecular Biology* 630 (2010): 271–299.

21. W. Ruan and M. Lai, "Actin, a Reliable Marker of Internal Control," *Clinica Chimica Acta* 385, no. 1 (2007): 1–5.

22. M. Greenwell and P. K. Rahman, "Medicinal Plants: Their Use in Anticancer Treatment," *International Journal of Pharmaceutical Sciences and Research* 6, no. 10 (2015): 4103–4112.

23. L. A. Smets, "Programmed Cell Death (Apoptosis) and Response to Anti-Cancer Drugs," *Anti-Cancer Drugs* 5, no. 1 (1994): 3–9.

24. A. Shamas-Din, J. Kale, B. Leber, and D. W. Andrews, "Mechanisms of Action of Bcl-2 Family Proteins," *Cold Spring Harbor Perspectives in Biology* 5, no. 4 (2013): a008714.

25. S. Qian, Z. Wei, W. Yang, J. Huang, Y. Yang, and J. Wang, "The Role of BCL-2 Family Proteins in Regulating Apoptosis and Cancer Therapy," *Frontiers in Oncology* 12 (2022): 985363.

26. B. Mansoori, A. Mohammadi, S. Davudian, S. Shirjang, and B. Baradaran, "The Different Mechanisms of Cancer Drug Resistance: A Brief Review," *Advanced Pharmaceutical Bulletin* 7, no. 3 (2017): 339–348.

27. A. B. Parrish, C. D. Freel, and S. Kornbluth, "Cellular Mechanisms Controlling Caspase Activation and Function," *Cold Spring Harbor Perspectives in Biology* 5, no. 6 (2013): a008672.

28. P. S. Mundi, J. Sachdev, C. McCourt, and K. Kalinsky, "AKT in Cancer: New Molecular Insights and Advances in Drug Development," *British Journal of Clinical Pharmacology* 82, no. 4 (2016): 943–956.

29. H. Pópulo, J. M. Lopes, and P. Soares, "The mTOR Signalling Pathway in Human Cancer," *International Journal of Molecular Sciences* 13, no. 2 (2012): 1886–1918.

30. R. S. Wong, "Apoptosis in Cancer: from Pathogenesis to Treatment," *Journal of Experimental & Clinical Cancer Research* 30, no. 1 (2011): 87.

31. B. S. P. M. Tolomeo and B. S. P. D. Simoni, "Drug Resistance and Apoptosis in Cancer Treatment: Development of New Apoptosis-Inducing Agents Active in Drug Resistant Malignancies," *Current Medicinal Chemistry-Anti-Cancer Agents* 2, no. 3 (2002): 387–401.

32. P. Sarantis, E. Koustas, A. Papadimitropoulou, A. G. Papavassiliou, and M. V. Karamouzis, "Pancreatic Ductal Adenocarcinoma: Treatment Hurdles, Tumor Microenvironment and Immunotherapy," *World Journal of Gastrointestinal Oncology* 12, no. 2 (2020): 173–181.

Supporting Information

Additional supporting information can be found online in the Supporting Information section.